

000
001
002
003
004
005
006
007
008
009
010
011

Abstract

Both consumer cameras and camera phones produce images that often exceed 10 megapixels. Yet computing and matching local features in images of this size can easily take more than twenty seconds using fast matching algorithms. This is much too slow for interactive applications and much too expensive for large scale image operations. We introduce Fast-Match, an algorithm designed to swiftly match large images without compromising on matching precision or recall. Fast-Match derives its speed from only computing features in those parts of the image that can be confidently matched. We show that Fast-Match is an order of magnitude faster than Ratio-Match, yet often doubles the precision on difficult to match image pairs at equal recall. In addition we prove that when one image is known in advance, Fast-Match can achieve linear performance $O(n)$ in the number of feature points n .

1. Introduction

Whenever we match local image features we are faced with a choice between performance and precision. On one hand SIFT features proposed by Lowe [1] have shown again and again to compare favorably to other local image descriptors, especially under unconstrained conditions such as perspective change with non-planar scenes [2–4]. On the other, SIFT keypoints and descriptors are slow to compute, the main *raison d'être* for the introduction of various alternative local image features. In many applications of computer vision we would like the increase the computational performance in order to work on larger images, bigger image sets, at faster frame rates or with more limited hardware, but we cannot give up the additional precision that SIFT affords us over other local features without negative effects for our application.

In this paper we introduce a matching algorithm designed to match features between two images only in image areas that are likely to correspond. This approach is much faster than traditional methods because there is no need to compute descriptors for areas in the image that are

not matched. We provide two variations of the algorithm: The *general* variation functions as a traditional matching algorithm and matches two unknown images albeit faster and more robustly than conventional methods. The *retrieval* variation on the other hand assumes that we know one of the images we intend to match beforehand; under this assumption, it can be a magnitude faster than existing matching methods without compromising on accuracy. We will unimaginatively refer to the proposed algorithm as *Fast-Match* in this paper and make clear from the context whether this refers to the *retrieval* or *general* variation.

The problem that *Fast-Match* attempts to solve is two-fold. By matching only image areas that are likely to correspond we hope to improve accuracy by entirely ignoring parts of the images that would otherwise likely be a source of incorrect correspondences. At the same time, this enables us to improve computational speed by not having to compute keypoints and descriptors for large parts of the images and at the same time reducing the amount of feature points we need to match. Both problems have been addressed in part by past work.

Fast-Match makes use of an angular assumption to efficiently find new matches in the geometric neighbourhood of already confirmed matches. However this constraint is only applied *locally* to increase the number of matches, making *Fast-Match* robust to outliers. In addition *Fast-Match* does not rely on an initial set of matches and derives much of its speed from the fact that not even an initial set of local image features is required.

This paper is structured as follows: Section 2 discuss related work. Section 3 introduces the *Fast-Match* algorithm. Section 4 outlines the experimental setup. In Section 5 we discuss the results before concluding in Section 6.

2. Related work

As noted, the cost of computing SIFT keypoints and descriptors is addressed by other local image features such as SURF [5], BRIEF [6], or BRISK [7], just to mention a few. Similarly efforts have been made to improve SIFT itself such as PCA-SIFT [8] and GLOH [2]. Both apply PCA to reduce descriptor lengths and improve distinctive-

108
109
110
111
112
113
114
115
116
117
118
119
120
121
122
123
124
125
126
127
128
129
130
131
ness, but neither have been shown to consistently outperform SIFT [2, 9].

132
133
134
135
136
137
138
139
140
141
142
Efforts to reduce the computational costs of finding nearest neighbours to feature points have largely focused on metric trees. Naively the set of nearest neighbours between features in two images can be computed by brute force in $O(n^2)$, where n is the total number of feature points in the two images (a typical three megapixel image may contain anywhere from 500 to 5000 feature points). When SIFT was originally published Lowe, proposed using the Best-Bin-First method to approximately search for nearest neighbours [10, 11]. This reduces the computational complexity to $O(n \log n)$, but even approximate metric trees are hard pressed to compete with brute force due to the high dimensionality of SIFT and the constant costs incurred with constructing and searching in a metric tree. Later work by Muja and Lowe [12] focused on improving approximate nearest neighbour searches by using several KD-Trees simultaneously while optimizing the tree structure using K-Means to cluster similar features. Recent work on knn-graphs shows a lot of promise for high dimensional cases [13]. We later review these improvements and their effect on efficiently matching large scale images.

143
144
145
146
147
148
149
150
151
152
A wealth of matching methods have focused instead on increasing the efficiency of local feature matching. *Fast-Match* builds upon the foundation of *Ratio-Match* introduced originally by Deriche et al. [14] and Baumberg [15] even though Lowe is usually credited for introducing it [1]. They both propose using the ratio of the similarity of the best to second best match of a given point to evaluate how unique it is. Their finding has later been tested by several independent teams, all concluding that thresholding based on this ratio is generally superior to thresholding based on similarity or returning all nearest neighbours [1–3, 16].

153
154
155
156
157
158
159
160
161
Brown and Lowe [17] extend ratio match to deal with a set of images by using not the ratio of the best and second best match, but the average ratio of the best and the average of second best matches across a set of images. Rabin et al. [16] try to enhance descriptor matching by looking at the statistical distribution of local features in the matched images, and only return a match when such a correspondence would not occur by mere chance. Finally, Arnfred et al. generalize *Ratio-Match* to make use of both of the matched images to provide a more accurate evaluation of the uniqueness of a match [18].

For sparse local image features many solutions have combined *Ratio-Match* with various geometric constraints to improve matching. These constraints are based on assumptions regarding the transformation between the *query* and *target images*. A commonly used example is *RANSAC* applied to feature matching where matches are chosen from a pool of candidates according to how well they approximate a global epipolar geometry [20–22]. Similar global



162
163
164
165
166
167
168
169
170
171
172
173
174
175
176
177
178
179
180
181
182
183
184
185
186
187
188
189
190
191
192
193
194
195
196
197
198
199
200
201
202
203
204
205
206
207
208
209
210
211
212
213
214
215
Figure 1: The 50 best matches by the proposed *Fast-Match* algorithm (left) and the *Ratio-Match* algorithm [1] (right). The lines between the image pairs denote a match as proposed by the algorithm. For *Fast-Match* the zones of the right image where local features were computed has been marked with a blue square.

angular and distance constraints can be used to filter a set of matches as shown in [23, 24]. Finally the problem of feature matching can be modelled as a graph matching problem where each feature is a vertex, and edge values correspond to a geometric relation between two features as demonstrated in [25–27]. For cases that require more flexibility such as scenes with moving elements and non-planar perspective change Pairwise constraints provide an alternative to the more rigid global constraints. Introduced by Leordeanu and Herbert [28], pairwise constraints work by applying a geometric constraint across matches on a pairwise basis, attempting to minimize the pairwise error. This approach has later been adopted by Pang et al. but made scale invariant and more efficient by using a voting scheme [29, 30]. Similarly we can cluster matches together based on a geometric constraint and treat each cluster as a separate case [31, 32]. An interesting application of this principle is demonstrated by Chen et al. who iteratively use a Hough transform to cluster matches using angular constraints [33].

While geometric constraints have been shown to work well, they are often susceptible to outliers and tend to be computationally demanding. All of the above geometric methods require a set of initial matches usually provided by *Ratio-Match* which acts as a lower bound on their running time. In practice even fast graph matching methods such as the covering trees method proposed by Yarkony et al. are two or three magnitudes slower than *Ratio-Match* [26].

3. Matching Fast and Slow

In this section we will introduce the fundamentals of *Fast-Match* and motivate the design choices as we go. The algorithm consists of 3 components; finding seeds, finding matches, and exploring for other places where matches might be.

3.1. Considerations

If we set out to design a truly fast matching algorithm, we cannot rely just on optimizing the matching step once the descriptors from both images have been found and com-

216
217
218
219
220
221
puted. Finding and computing descriptors can easily account for 80% of the time spent matching for bigger images (cf. Figure 7). For this reason *Fast-Match* is designed to only compute features for the part of the image we hope to match.

222
223
224
225
226
227
228
229
230
231
232
233
234
235
236
The *Fast-Match* algorithm is demonstrated in Algorithm 1. Given a *query image* and a *target image* that we intend to match and a confidence threshold τ , we obtain a set of seed matches from the two images. For each seed match we look at the matched position in the *query* and *target images* and find a set of matches. We save these matches and their confidence scores; for those that pass the confidence threshold τ , we obtain another set of seed matches. In this way we iterate until we have no more seed matches and return the matches and their confidence scores. In an intuitive sense τ serves as a parameter directing the thoroughness of the algorithm, i.e. how much time we spend matching, while the final precision and recall can be adjusted by thresholding the matches on their confidence scores at the end.

237
238
239
240
241
242
We a *general* and a *retrieval* variation of the algorithm. The latter assumes that we know one of the images that we intend to match ahead of time and can do some off-line computations. For the *general* variation we make those computations on the fly instead and do not assume anything to be pre-computed.

243 244 **Algorithm 1** Fast-Match

245
Require: $I_{\text{query}}, I_{\text{target}}$: images, $\text{maxiter} \in \mathbb{N}, \tau \in [0, 1]$
246 $M_{\text{seed}} \leftarrow \text{seed_matches}(I_{\text{query}}, I_{\text{target}})$
247 $M_{\text{final}} \leftarrow \emptyset$
248 $C_{\text{final}} \leftarrow \emptyset$
249 $M_{\text{seen}} \leftarrow \emptyset$
250 **while** $M_{\text{seed}} \neq \emptyset \wedge i < \text{maxiter}$ **do**
251 $M_{\text{round}} \leftarrow \text{get_matches}(M_{\text{seed}})$
252 $C_{\text{round}} \leftarrow \text{get_confidence}(M_{\text{round}})$
253 $M_{\text{seed}} \leftarrow \text{get_seeds}(M_{\text{round}} \setminus M_{\text{seen}}, C_{\text{round}}, \tau)$
254 $M_{\text{seen}} \leftarrow M_{\text{seen}} \cup M_{\text{seed}}$
255 $M_{\text{final}} \leftarrow M_{\text{final}} \cup M_{\text{round}}$
256 $C_{\text{final}} \leftarrow C_{\text{final}} \cup C_{\text{round}}$
257 **end while**
258 **return** $M_{\text{final}}, C_{\text{final}}$

261 3.2. Initiating Seeds

262
263
Depending on the scenario, several strategies can be used to obtain a set of initial seed matches. In practice we have found it efficient to resize both images to thumbnails and use *Ratio-Match* to obtain a set of matches and ratios that we then threshold with the confidence threshold τ to obtain the initial seed matches. The thumbnails created need to be sized so they on one hand ensure that objects of interest are

270
271
272
273
274
275
still detectable by a keypoint detector while on the other remain small to ensure that we find matches efficiently. We determine empirically that a thumbnail size of 300×300 pixels maintains a good balance between speed and accuracy. We found this size to be independent of the original image size as long as we are matching images that are bigger than one megapixel.

276 277 3.3. Collecting Matches and Computing Confidence

278
279
280
281
282
283
284
285
If a seed match yields a connection between two points p_q in the *query image* and p_t in the *target image*, then we are interested in collecting all matches between the regions R_q and R_t centered around p_q and p_t respectively. From each region we can extract a set of feature points between which we try to find a set of matches M_{qt} and a set of confidence scores C_{qt} .

286
287
288
289
290
Lowe and others have shown that the distance between two SIFT descriptors is much less indicative of a true correspondence than the ratio between the best and second best match [1–3, 16]. This ratio is more formally defined as follows: If we let f_q be a feature in the *query image* and f_t, f_b be the two nearest neighbours of f_q in the *target image* then the ratio r is defined as follows:

$$r = \frac{d(f_q, f_t)}{d(f_q, f_b)}.$$

291
292
293
294
295
296
Here $d(f_i, f_j)$ is the distance between the features f_i and f_j . For SIFT this is the Euclidean distance. The distance between two feature points is greater when the feature points resemble each other less. For this reason we have higher confidence in a match with a low r -value. Using r as a measure of match confidence presumes that we expect each feature in the *target image* to have at most one true correspondence in the *target image*. Intuitively if we try to find a match for a feature f_i in an image that does not have any true correspondences, then we would expect the two closest neighbours to be roughly equally well matched with f_i . For this reason we attribute high confidence to matches where the closest neighbour is dramatically closer to f_i than the second closest neighbour and discard the rest.

297
298
299
300
301
302
303
304
305
306
307
308
309
310
We are faced with a problem when applying this technique to obtain the set of confidence scores C_{qt} , since for any match in M_{qt} we only know the nearest neighbours amongst the features of R_q and R_t . To get around this problem we either assume to know one of the images beforehand (the *retrieval* variation) or – in case we cannot make that assumption – we compute the features of one of the images (the *general* variation). For a given match between features f_q and f_t we can now find the second closest neighbour f_b and calculate the confidence as $r = d(f_q, f_t)/d(f_q, f_b)$.

311
312
313
314
315
316
317
318
319
320
321
In the retrieval scenario where we know an image beforehand, we can further optimize this step. If we assume

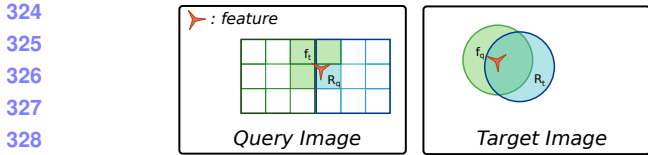


Figure 2: Exploration of features based on match. The areas shaded blue are the areas that were searched to obtain the match. The areas shaded green are candidate areas for obtaining more matches.

the *target image* is known in advance we can approximate the ratio by letting $\hat{r} = d(f_t, f_q)/d(f_t, f_b)$. Here the feature f_b is also part of the target image, which means we can pre-calculate $d(f_t, f_b)$ for all features in the cached *target image* before we start matching. When these distances are tied to their corresponding feature in the target image, it becomes trivial to calculate \hat{r} .

3.4. Exploring for Matches

In each iteration we compute a new set of seed matches, i.e. positions that might yield more matches in the image. For each region R_i evaluated during the collection step we now have a set of matches M_i and a set of confidence levels C_i that we can use to predict whether the neighbourhood of R_i is worth exploring.

There are many possible heuristics for predicting possible regions including local and global epipolar assumptions and partial graph isomorphisms. However, for the sake of simplicity and speed we have chosen a straightforward approach based on weak angular assumptions, as illustrated in Figure 2. Assuming that the *target image* has been cached either in advance or before the matching step, the blue shaded areas show R_q and R_t for a given seed match. In the *target image* we collect all features in a given radius while we compute features in the rectangular R_q in the *query image*. For performance reasons we compute all features in the blue square but match only the features inside the shaded area. Next a match is found in the collection step between f_q and f_t . Based on the position of f_q in R_q we select three areas with potential for more matches. The center of each is matched with the center position f_t to produce three seed matches for the next iteration. In Figure 1 we illustrate this process in the *Fast-Match* image pair. The *query image* to the right in the figure has a small blue square for each region that has been used while matching the two images.

In practice it is necessary that these squares overlap in order to detect features lying close to the edges. This incurs a bit of overhead which is minimized by only collecting features for groups of 9 squares. In order to avoid computing the same matches or features twice, quite a bit of care has to be expended making sure that results are properly cached.

A matrix containing ‘bins’ of features can conveniently be used to store features from different image regions. Similarly a hash-set is suitable for keeping track of which regions have already been matched and which matches have already been found.

3.5. Computational Complexity

The difference between the *general* and *retrieval* variation of *Fast-Match* consists in whether we compute the features in the *target image* (general) or if we presume the features are computed offline (retrieval). Computing the features is linear in the number of feature points, while finding $d(f_q, f_b)$ for all n features in the *target image* can be done in $O(n \log n)$ using metric trees.

Once the features and their distances have been computed, the algorithm iteratively finds new seed matches based on previous sets of seed matches. For each seed match we collect new matches, calculate confidence scores, and obtain new seed matches. Each of these steps varies only with the local region size which is constant. As a consequence the running time is linear in the amount of possible seed matches.

We will show that the number of possible seed matches is on average linear in the number of image features, and we also provide an upper bound for the probability that it is not. We assume that outside of true correspondences, features have better or at least equally good matches in terms of confidence in the image they come from. More rigorously put: For any feature in the *target image* f_t let f_1, f_2, \dots be the best, second best, etc matching feature from either image which is not a true correspondence. Let A_{ti} be the event that f_i is found in the *query image*, then $\mathbb{P}(A_{ti}) \leq 0.5$ and A_{ti} is independent from A_{tj} when $i \neq j$.

For a given feature in the *target image* f_t , its nearest neighbour in the *target image* f_b , and the set of features in the *query image* F_{query} , we can define the stochastic variable X_t as follows:

$$X_t = |\{f_q \mid f_q \in F_{query}, d(f_q, f_t) < d(f_q, f_b)\}| \quad (1)$$

That is, X_t is the number of features in the query image closer to f_q than f_b . For each feature f_t , X_t is an i.i.d. stochastic variable.

In the worst case, each feature in the *target image* has a true correspondence in the *query image* and $\mathbb{P}(A_{ti} = 0.5)$, in which case we find can find $\mathbb{P}(X_t = n) = \mathbb{P}(A_{ti})^n = 0.5^n$, as well as the expected value $\mathbb{E}(X_t) = \sum_{i=1}^{\infty} i 0.5^i = 2$, and the variance $Var(X_t) = \sum_{i=1}^{\infty} 0.5^i (i - 2)^2 = 6$.

For $\tau = 1$ we accept a seed match when $d(f_t, f_q) \leq d(f_t, f_b)$. That means that for any feature in the *query image*, we accept at most X_t matches. To find the total amount of seed matches given n , we let $S_n = X_1 + \dots + X_n$, in which case $\mathbb{E}(S_n) = 2n$. This proves that the expected

378

379

380

381

382

383

384

385

386

387

388

389

390

391

392

393

394

395

396

397

398

399

400

401

402

403

404

405

406

407

408

409

410

411

412

413

414

415

416

417

418

419

420

421

422

423

424

425

426

427

428

429

430

431

amount of seed matches is linear in the number of target features.

For the above case it is theoretically possible that for every one of the n features we end up considering kn seed matches for some constant k , i.e. a quadratic behaviour. Using Chebyshev's inequality we can provide an upper bound on the probability of this event:

$$\mathbb{P}\left(\left|\frac{S_n}{n} - \mathbb{E}(X_t)\right| \geq kn\right) \leq \frac{\text{Var}\left(\frac{S_n}{n}\right)}{k^2 n^2} = \frac{6}{k^2 n^3} \quad (2)$$

It is clear that for any constant k we can pick a number of features n which render the likelihood of a quadratic behaviour infinitesimal. In essence the larger n becomes, the less likely *Fast-Match* is to exhibit super linear behaviour.

The noteworthy part of this result is that for the *retrieval* variation we can match two images in $O(n)$. Since there are no large constants involved this makes it possible to rapidly match very large images. In particular *Fast-Match* is suited for cases where we are looking to match several large *query images* to one *target image*. In this case we can compute the features and distances of the *target image* and then match each *query image* in linear time. In contrast the general variation still has a complexity of $O(n \log n)$ due to the necessity of calculating distances online.

4. Experimental Setup

To evaluate *Fast-Match* on three sets of data. We use a dataset of 3024 image pairs featuring various 3D objects at different angles and lighting conditions to measure matching performance for real life objects when lighting and perspective changes. To evaluate the performance of *Fast-Match* when only part of (or none of) the scene is shared between an image pair we conduct experiments on 400 random crops with different degree of image overlap taken from 4 image pairs, creating a challenging test set where large part of the images consists of background clutter similar in nature to the subject being matched. Finally we time the algorithm on two pairs of images with high pixel counts to measure performance in terms of speed.

We compare the algorithm to the standard *Ratio-Match* [1] as well as the newer *Mirror-Match* [18]. We exclude the geometric algorithms discussed in related works from comparison because even the fastest cases are two to three magnitudes slower than *Ratio-Match* and as such are too time consuming to use when matching features in large images.

4.1. Evaluation of Fast-Match on 3D Objects

The 3D Objects dataset by Moreels and Perona [3] allows us to experimentally compare matching algorithms over a large range of object and surface types rotated on a turnstile and photographed from every angle in increments of 5 degrees. 15 objects from the dataset are shown in Figure 3. We use images of 84 different objects photographed

under three different lighting conditions at 12 different angle intervals, conducting experiments with a total of 3024 image pairs. All photos a taken with a consumer camera in 3.1 megapixel resolution.

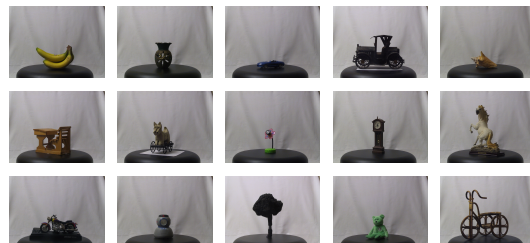


Figure 3: 15 objects from the 3D Objects dataset by Moreels and Pietro [3].

To validate matches, Moreels and Perona propose a method using epipolar constraints [3, p.266]. According to their experiments, these constraints are able to identify true correspondences with an error rate of 2%. We use their proposed method to generate the ground truth for the evaluation of our framework.

To compute the total number of possible true correspondences, we take each feature in a *query image* and count how many of them have a feature in the *target image* which would satisfy the epipolar constraints. To avoid matching non-moving background and foreground objects we excluded features with no correspondences from being matched. This was necessary because a relatively small number of actual true correspondences between folds in the background material were mistakenly counted as false positives when evaluated which impacted the precision of test in particular on cases with few true correspondences. In practice only few feature points were excluded for this reason.

We evaluate all matching algorithms from our framework on the 3D Objects dataset by matching images at different angular intervals. For each object we pick the *query image* as the image taken at 10 degrees rotation for calibration stability. We then match this image with the same object turned an additional Δ degrees, $\Delta \in \{5, 10, \dots, 60\}$. For every angle interval we compare images taken under 3 different lighting conditions as provided by the dataset. We include all objects in the database for which photos at 5 degree angle intervals are available except for the "Rooster" and "Sponge" objects due to image irregularities. For each angle this means that a total of 252 image pairs are matched. We calculate the result these pairs using a weighted average based on the number of actual correspondences for each pairs. This ensures that image pairs that are more difficult to match are not contributing less to the end result because less actual matches would be found.

540
541 **4.2. Evaluation of Fast-Match on partially overlap-**
542 **ping scenes**



551
552 Figure 4: Four image pairs from the Graffiti dataset by
553 Mikolajczyk et al. [2]. From left to right the images are
554 ‘Boat’, ‘Graf’, ‘Bark’ and ‘Wall’.

555 To evaluate how well *Fast-Match* handles partially overlap-
556 ping scenes we make use of four images from the Gra-
557 fitti dataset by Mikolajczyk et al. [2] as displayed in Figure
558 4 all featuring challenging perspective change. For each of
559 the four image pairs we generate a hundred pairs of smaller
560 crops each crop randomly positioned within the original im-
561 age. This process ensures that image pairs that does not
562 contain any overlap in scene are still visually similar, mak-
563 ing it more challenging for a matching algorithm to avoid
564 false positives, i.e. matching local image features that are
565 not true correspondences.

566 In practice the amount of overlap between pairs in a test
567 set will depend on the overlap and viewpoint change in the
568 source image pair. To give a rough idea, Table 1 shows the
569 overlap of patch pairs created from images 1 and 3 of the
570 *Graf* image.

572 Table 1: Overlap in the set of 100 patch pairs created from
573 the ‘Graf’ image pair (Figure 4).

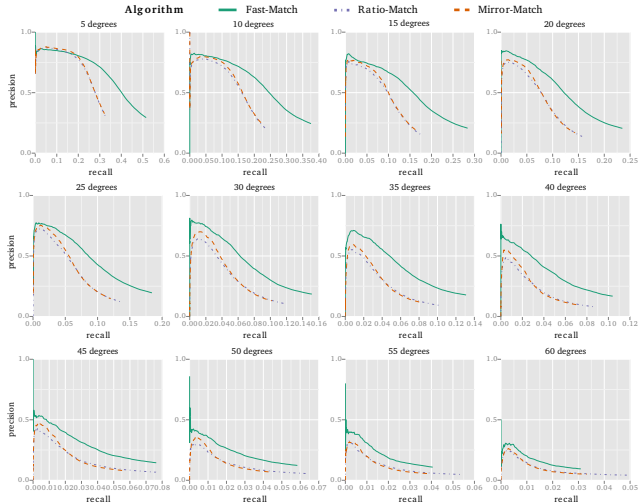
Amount of overlap:	0%	< 50%	> 50%
Number of patch pairs:	21	54	25

578 Given a potential match between two pixels p_1 and p_2 ,
579 $m = (p_1, p_2)$, and a homography H relating the two images
580 I_1 and I_2 , we can calculate if m is an inlier by checking if
581 the two points satisfy the following criteria:

$$|Hp_1 - p_2| + |H^{-1}p_2 - p_1| < d_{\max}$$

585 That is, the distance between p_1 translated to I_2 and p_2 plus
586 the distance between p_2 translated to I_1 should be less than
587 a certain threshold (we use $d_{\max} = 5$ pixels here).

588 As with the 3D Objects we accumulate results across the
589 hundred image crop pairs by using an average weighted by
590 the amount of true correspondences between each cropped
591 pair. This ensures that difficult to match and trivial image
592 pairs have an equal impact on the evaluation result despite
593 the difficult image pairs yielding far less actual matches.



594
595 Figure 5: Results for the 3D Objects dataset. Each plot con-
596 tains the average precision and recall over 84 objects photo-
597 graphed under 3 different lighting conditions weighted
598 over the number of true correspondences for each pair.

600
601 **4.3. Configuration of Fast-Match**

602 The central parameters of *Fast-Match* are the confidence
603 threshold τ for selecting seed matches and the final con-
604 fidence threshold applied to the total set of matches. For
605 the experiments we let $\tau = 0.9$ and created precision/recall
606 plots by varying the confidence threshold over the final set
607 of matches.

608 To achieve a good balance between speed and robustness
609 we let the region in which we extract features be a square
610 window with a side length of 90 pixels. From empirical
611 tests we found that this number works well with the SIFT
612 feature descriptor, but for other descriptors different num-
613 bers might lead to better performance. The window is split
614 in to nine smaller squares (see also Figure 2). When a seed
615 match falls in any of these squares we match only the fea-
616 tures within the smaller square. We let both the regions and
617 the smaller squares overlap each other at all edges with 25
618 pixels in order to capture feature points lying close to an
619 edge. For the image we have already cached we find all
620 features within a radius of 50 pixels of the seed match.

621 **5. Results**

622 Figure 5 shows the performance of the different match-
623 ing methods in our proposed framework for 12 increas-
624 ingly bigger angle differences. The results are shown in
625 a precision-recall plot to make it easy to compare perfor-
626 mance in terms of precision at similar levels of recall. For
627 each plot we show the accumulated results on all 3D ob-
628 jects, weighted by the number of possible true correspon-
629 dences for the individual objects. This ensures that each ob-

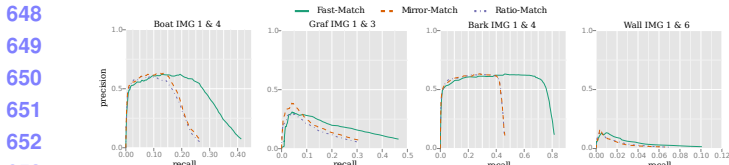


Figure 6: Results for the Graffiti dataset. Each plot contains the average result over 100 semi overlapping image patches based on the same two images weighted over the number of true correspondences for each pair.

ject contributes equally to the final result, despite some objects resulting in disproportionately more matches than others.

At low angular differences all algorithms show similar performance at low recall, however *Fast-Match* is superior to *Ratio-Match* and *Mirror-Match* at higher recall, more than doubling the precision at similar recall levels. This picture remains the same at higher angular differences, but with a higher performance gap between *Fast-Match* and the other algorithms at low recall while more than doubling precision at higher recalls. For image pairs with angular differences of more than 40° the performance of all algorithms declines, with *Fast-Match* still coming out on top.

The high recall rates of *Fast-Match* are partially explained by the fact that we can allow our confidence thresholds to be more lenient when we already know that we are likely to find true correspondences in the regions that we are matching. However, lenient thresholds can easily impact the matching speed, so in practical situations we usually have to choose between matching fast and precisely, or more slowly with higher recall.

In Figure 6 we see the performance of the three different matching methods over 400 crop pairs based on four image pairs. As for the 3D Objects the results are shown in a precision-recall plot weighted by the number of possible true correspondences for the individual crop pairs.

At low recall we see a similar performance across all algorithms, but as the algorithms return more matches, *Fast-Match* shows drastically better precision at similar recall levels than *Mirror-Match* and *Ratio-Match*. While this difference is more noticeable in the case of the ‘Bark’ and ‘Boat’ images, the ‘Graf’ and ‘Wall’ also see a drastic improvement in recall but as precision is lower in general for these two images the effect is less visible.

For all four image pairs we see a precision dip at very low recall which is explained by the presence of image crop pairs with no or little overlap. When matching these pairs we might often find matches even though there are no or few possible true correspondences which in effect negatively impacts the results at very low recall rates.

Figure 7 demonstrate the speed of *Fast-Match* on image sizes as is typically produced by modern consumer cameras

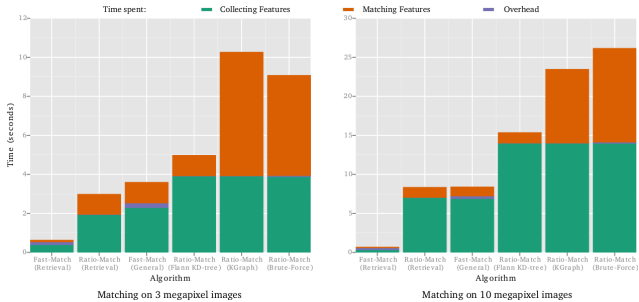


Figure 7: The duration in seconds of different variations of *Fast-Match* and *Ratio-Match*. The top plot shows results for two 10 MPixel images two 3 Mpixel images is used for the comparison at the bottom. From the left, the first two results presume a precached image while the rest do not require knowing any inputs beforehand. The image pairs used can be seen in Figure 1

and camera phones. In Figure 7 we compare the speed of the two variations of *Fast-Match* to different variations of *Ratio-Match* on two image pairs, one with two images of 10 megapixel and another where the same image pair has been scaled to 3 megapixels. For the larger images we see the clearest difference in performance. The retrieval variant of *Fast-Match* matches the image pairs in around one second while a retrieval variant of *Ratio-Match* with pre-computed features spends eight seconds on the same task. This result is roughly equal to the time the general variation of *Fast-Match* spends matching the two images without any pre-computations. For the nearest neighbor search we note that for large images there are substantial speed gains to be had by choosing the right algorithm for finding nearest neighbors, with Muja et al.’s Flann matcher being vastly superior to brute force and KGraph.

For the 3 megapixel picture the pattern repeats itself, although with smaller margins separating *Fast-Match* and *Ratio-Match*. When images are smaller, computations like obtaining the initial seed matches are comparatively more costly.

Figure 1 shows the result from matching the pair of three megapixel images using *Fast-Match* and *Ratio-Match*. *Fast-Match* ends up only matching the part of the images that are likely to have correspondences. This highlights both a strength and a weakness of *Fast-Match*. It is this myopic matching approach that is responsible for *Fast-Match*’ speed and precision; on the other hand, *Fast-Match* is not the best candidate for images that are almost identical, because its step by step approach incurs too much overhead to compete in speed with *Ratio-Match* in those cases.

756

757

758

759

760

761

762

763

764

765

766

767

768

769

770

771

772

773

774

775

776

777

778

779

780

781

782

783

784

785

786

787

788

789

790

791

792

793

794

795

796

797

798

799

800

801

802

803

804

805

806

807

808

809

6. Conclusion

We have introduced *Fast-Match* in two forms, a general and a retrieval variation. The retrieval variation assumes that we know one of the images that we are matching ahead of time in order to pre-cache feature points. The general variation has no assumptions and performs the pre-caching of feature points online instead. We have proven that while the general variation has a computational complexity of $O(n \log n)$ with n being the number of feature points, the retrieval variation will on average run in $O(n)$. From experiments on large images we have shown that *Fast-Match* can be a magnitude faster than *Ratio-Match* while providing comparable results. We further compared *Fast-Match* to *Ratio-Match* and *Mirror-Match* using images of rotated 3D objects to demonstrate that *Fast-Match* outperforms the other algorithms significantly over 3024 image pairs and in most cases doubles the matching precision at similar recall rates. We show that these results hold true for matching cases featuring partial or no overlap by comparing *Fast-Match* on 400 crop pairs of planar scenes. *Fast-Match* is particularly applicable in cases where we are interested in matching one image to multiple large images, in which case we can quickly pre-cache the image and use this data for each of the other images.

References

- [1] Lowe, D.G.: Distinctive image features from scale-invariant keypoints. *International Journal on Computer Vision* **60** (2004) 91–110
- [2] Mikolajczyk, K., Schmid, C.: A performance evaluation of local descriptors. *IEEE Trans. Pattern Analysis and Machine Intelligence* **27** (2005) 1615–1630
- [3] Moreels, P., Perona, P.: Evaluation of features detectors and descriptors based on 3D objects. *International Journal on Computer Vision* **73** (2007) 263–284
- [4] Heinly, J., Dunn, E., Frahm, J.M.: Comparative evaluation of binary features. In: Proc. European Conference on Computer Vision (ECCV). (2012) 759–773
- [5] Bay, H., Tuytelaars, T., Van Gool, L.: SURF: Speeded up robust features. In: Proc. European Conference on Computer Vision (ECCV). (2006) 404–417
- [6] Calonder, M., Lepetit, V., Strecha, C., Fua, P.: BRIEF: binary robust independent elementary features. In: Proc. European Conference on Computer Vision (ECCV). (2010) 778–792
- [7] Leutenegger, S., Chli, M., Siegwart, R.Y.: BRISK: Binary robust invariant scalable keypoints. In: Proc. International Conference on Computer Vision (ICCV), IEEE (2011) 2548–2555
- [8] Ke, Y., Sukthankar, R.: PCA-SIFT: A more distinctive representation for local image descriptors. In: Proc. IEEE Conference on Computer Vision and Pattern Recognition (CVPR). Volume 2., IEEE (2004) II–506
- [9] Li, J., Allinson, N.M.: A comprehensive review of current local features for computer vision. *Neurocomputing* **71** (2008) 1771–1787
- [10] Beis, J.S., Lowe, D.G.: Shape indexing using approximate nearest-neighbour search in high-dimensional spaces. In: Computer Vision and Pattern Recognition, 1997. Proceedings., 1997 IEEE Computer Society Conference on, IEEE (1997) 1000–1006
- [11] Lowe, D.G.: Object recognition from local scale-invariant features. In: Computer vision, 1999. The proceedings of the seventh IEEE international conference on. Volume 2., Ieee (1999) 1150–1157
- [12] Muja, M., Lowe, D.G.: Fast approximate nearest neighbors with automatic algorithm configuration. In: VISAPP (1). (2009) 331–340
- [13] Dong, W., Moses, C., Li, K.: Efficient k-nearest neighbor graph construction for generic similarity measures. In: Proceedings of the 20th international conference on World wide web, ACM (2011) 577–586
- [14] Deriche, R., Zhang, Z., Luong, Q.T., Faugeras, O.: Robust recovery of the epipolar geometry for an uncalibrated stereo rig. In: Proc. European Conference on Computer Vision (ECCV). (1994) 567–576
- [15] Baumberg, A.: Reliable feature matching across widely separated views. In: Proc. IEEE Conference on Computer Vision and Pattern Recognition (CVPR). Volume 1. (2000) 774–781
- [16] Rabin, J., Delon, J., Gousseau, Y.: A statistical approach to the matching of local features. *SIAM Journal on Imaging Sciences* **2** (2009) 931–958
- [17] Brown, M., Szeliski, R., Winder, S.: Multi-image matching using multi-scale oriented patches. In: Proc. IEEE Conference on Computer Vision and Pattern Recognition (CVPR). Volume 1. (2005) 510–517
- [18] Arnfred, J.T., Winkler, S., Süsstrunk, S.: Mirror Match: Reliable feature point matching without geometric constraints. In: Proc. IAPR Asian Conference on Pattern Recognition (ACPR). (2013) 256–260
- [19] Barnes, C., Shechtman, E., Finkelstein, A., Goldman, D.: PatchMatch: a randomized correspondence algorithm for structural image editing. *ACM Transactions on Graphics-TOG* **28** (2009) 24

810
811
812
813
814
815
816
817
818
819
820
821
822
823
824
825
826
827
828
829
830
831
832
833
834
835
836
837
838
839
840
841
842
843
844
845
846
847
848
849
850
851
852
853
854
855
856
857
858
859
860
861
862
863

- 864 [20] Fischler, M.A., Bolles, R.C.: Random sample consensus: a paradigm for model fitting with applications to
865 image analysis and automated cartography. Communications of the ACM **24** (1981) 381–395 918
866
867
868
869 [21] Torr, P.H.S., Zisserman, A.: MLESAC: A new robust 919
870 estimator with application to estimating image geometry. Computer Vision and Image Understanding **78** 920
871 (2000) 138–156 921
872
873 [22] Szeliski, R.: Computer Vision: Algorithms and Applications. Springer (2010) 922
874
875
876 [23] Kim, J., Choi, O., Kweon, I.S.: Efficient feature 923
877 tracking for scene recognition using angular and scale 924
878 constraints. In: Proc. IEEE/RSJ International Conference 925
879 on Intelligent Robots and Systems (IROS), Nice, 926
880 France (2008) 4086–4091 927
881
882 [24] Schmid, C., Mohr, R.: Local grayvalue invariants for 928
883 image retrieval. IEEE Transactions on Pattern Analysis 929
884 and Machine Intelligence **19** (1997) 530–535 930
885
886 [25] Torresani, L., Kolmogorov, V., Rother, C.: Feature 931
887 correspondence via graph matching: Models and 932
888 global optimization. In: Proc. European Conference 933
889 on Computer Vision (ECCV). Springer (2008) 596– 934
609 935
890
891 [26] Yarkony, J., Fowlkes, C., Ihler, A.: Covering trees 936
892 and lower-bounds on quadratic assignment. In: Proc. 937
893 IEEE Conference on Computer Vision and Pattern 938
894 Recognition (CVPR), IEEE (2010) 887–894 939
895
896 [27] Cho, M., Lee, J., Lee, K.M.: Reweighted random 940
897 walks for graph matching. In: Proc. European Conference 941
898 on Computer Vision (ECCV). Springer (2010) 942
492–505 943
899
900 [28] Leordeanu, M., Hebert, M.: A spectral technique for 944
901 correspondence problems using pairwise constraints. 945
902 In: Proc. IEEE Conference on Computer Vision and 946
903 Pattern Recognition (CVPR). Volume 2., San Diego, 947
904 CA (2005) 1482–1489 948
905
906 [29] Yuan, Y., Pang, Y., Wang, K., Shang, M.: Efficient 949
907 image matching using weighted voting. Pattern Recognition Letters **33** (2012) 471–475 950
908
909 [30] Pang, Y., Shang, M., Yuan, Y., Pan, J.: Scale 951
910 invariant image matching using triplewise constraint and 952
911 weighted voting. Neurocomputing **83** (2012) 64–71 953
912
913 [31] Cho, M., Lee, J., Lee, K.M.: Feature correspondence 954
914 and deformable object matching via agglomerative 955
915 correspondence clustering. In: Proc. International 956
916 Conference on Computer Vision (ICCV), IEEE (2009) 957
1280–1287 958
917